Paperboard Forming - Specifics Compared to Sheet Metal Forming

Peter Groche* and Dominik Huttel

Growing demand for sustainable products has led to increased interest in the use of paperboard as a structural material. Paperboard products are almost exclusively manufactured by embossing, pulp molding, and bending processes. Other well-known forming methods, such as deep or stretch drawing, are only rarely applied to paperboard. This is primarily ascribed to the lack of knowledge concerning the process design and limits when paperboard is employed. In the present work, the applicability of well-established design strategies and characterization methods for metals to paperboard is investigated. Therefore, forming limit diagrams for paperboard are determined in a first step. Additionally, significant material parameters are identified in order to describe the material influence upon the forming limit. Furthermore, the influence of a hydrostatic counter pressure onto the forming limit is investigated. To predict the forming behaviour of a complex formed paperboard demonstration part, a numerical model of a hydroforming process is set up, executed, and validated.

Keywords: Hydroforming; Modelling; Paperboard

*Contact information: Institute for Forming Technology and Machines, Technische Universität Darmstadt, Germany; *Corresponding author: groche@ptu.tu-darmstadt.de*

INTRODUCTION

Life-cycle analyses of paperboard products reveal their attractiveness: the basic fibrous material is renewable, manufactured efficiently in large-scale production processes, light, and recyclable. Furthermore, the properties of paperboard, like its density, strength, surface roughness, and porosity, can be adjusted to meet a wide range of different requirements with the appropriate mechanical treatment, chemical composition, production process parameters, and environmental conditions (Xia 2002; Alava and Niskanen 2006).

Paperboard products with developable surfaces, such as plates or folding boxes, are frequently used. More complex, three-dimensional, hollow parts made of paperboard are rare and are produced by pulp moulding, if at all. Other processes, such as deep or stretch drawing, which are well-established for forming metals, are not common in industrial paperboard production. To make use of the advantageous potential of these processes for paperboard, an expansion of production technologies is necessary.

Compared to sheet metal, huge deficits exist in terms of constitutive material and friction modelling, characterisation methods, and process technology when deep or stretch drawing should be applied to paperboard. A closer look at metal (DC04 – common deep drawing alloy) and paperboard, as shown in Fig. 1, exhibits the differences in their microscopic structure. Metal consists of a lattice structure. Plastic deformation is enabled by the movement of atomic layers. This is eased by the movement of dislocations, as displayed in Fig. 1a. Paperboard consists of fibres connected by hydrogen

bonds. These bonds primarily determine the strength of the fibre network (Davidson 1972). Irreversible deformation of paperboard is attributed to the distortion of the web, the stretching of curled fibres, and the movement of the fibres in the web. The last deformation mechanism is associated with a release and reshuffling of hydrogen bonds in the web. A schematic of the irreversible deformation of paperboard is shown in Fig. 1b.

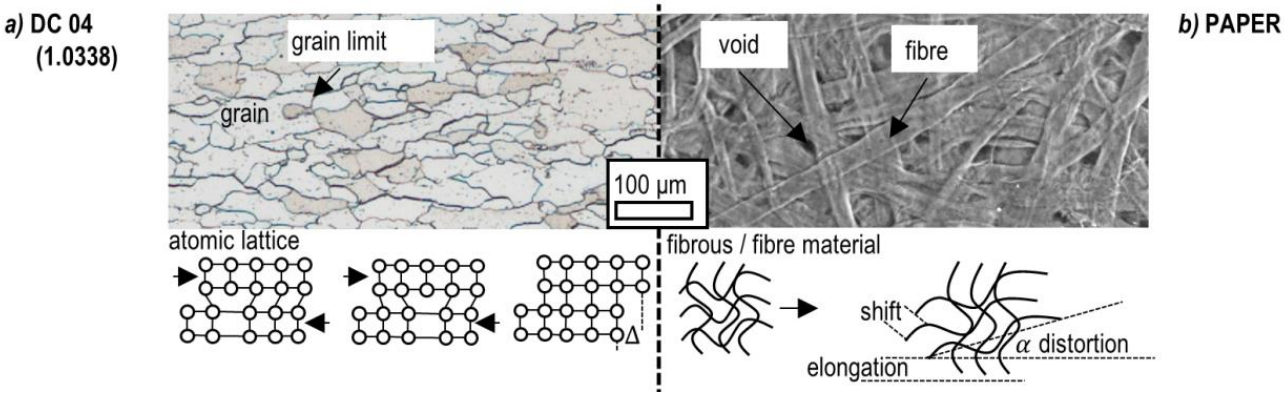

Fig. 1. a) Grinding surface pattern of DC04 and forming mechanisms of metal according to Weißbach (2007); b) surface of paperboard and forming mechanisms

An overview of material testing and modelling methods, as given for sheet metal (Bruschi *et al.* 2014), is not available for paperboard. Different authors have focused their research on modelling strategies for paper and paperboard. They have attempted to find a reasonable trade-off between model complexity, the effort necessary for parameter determination, and the reliability of the model predictions. Several researchers have chosen modelling strategies based on simplified models with a reduced amount of parameters. Mäkela and Östlund (2003) were able to predict paperboard's behaviour in tensile tests using an orthotropic, elastic-plastic material model with associated plasticity.

In the case of corrugated board boxes under load, in addition to the complex material behaviour, the geometry of the wall structure must be modelled. Jiménez-Caballero *et al.* (2009) predicted the deformation characteristics by modelling the corrugated wall structure and by the use of an orthotropic material model, including damage and different behaviours in tension and compression. To describe the behaviour of paperboard in the case of large deformations, as well as for fracturing processes, enhanced modelling strategies are used. The damaging of paperboard material is considered to be a sequence of crack initiation, growth, and crack coalescence. Material laws describing these mechanisms include damage variables and damage evolution laws. Isaksson *et al*. (2004) represented experimental tensile test results through the combination of the damage behaviour and anisotropy of the material by the concept of Hill (1948). According to Xia (2002), the behaviour of paperboard creasing and folding processes can be represented as a yield surface build up by sub-surfaces. Hereby, the anisotropic behaviour, in combination with an associated flow rule, is taken into account. The paperboard is represented as a multi-layer structure. An interface model, including damage associated with the inelastic history of the interface displacement, describes the out-of-plane delamination. The model is capable of describing the experimentally observed delamination behaviour during creasing and folding processes as well as the correlations between the bending moment and bending angle (Xia 2002). Further enhancement of the interface model has allowed for enhanced correlation between

simulations and experimental results (Nygards *et al.* 2009). Huang (2013) concluded that a simplification of the modelling strategy using Hill's concept for anisotropic material behaviour, in combination with the multi-layer structure, allowed for realistic prediction of the force *versus* displacement curves of creasing and folding processes. Neglecting the layer structure in the case of deep drawing processes yields comparable results. Further simplifications using a shell modelling strategy instead of volumetric elements exhibited deviations compared to other modelling strategies (Huang 2006). Validation of material models is difficult given the lack of measured strain distributions available in the present literature.

To predict the deformation limits given by the occurrence of cracks, the constitutive formulation of Lemaitre and Desmorat (2005) can be used to describe the paperboard degeneration. Material damage can be determined by acoustic emission testing (Isaksson *et al.* 2006). Other methods for the prediction of cracks, like forming limit diagrams (FLD) (Bruschi *et al*. 2014), have not yet been used for paperboard. The increase in hydrostatic pressure has been proven an adequate measure to expand the formability limits of sheet metal forming (Groche *et al*. 2002). Until now, it has been unknown how effective this measure is for paperboard forming.

It is well recognised that the result of a forming process is strongly affected by friction between workpiece and tools. Relative velocities between 0 and 120 mm/s, normal pressures in the range of 0 and 1 N/mm², and moisture contents of up to 15% are the typical tribological conditions during the deep and stretch drawing of paperboard (Scherer 1935; Hauptmann 2010; Östlund *et al*. 2011; Vishtal *et al*. 2014). The friction coefficient decreases with increasing temperature (Back 1991). In this context, differences between static and dynamic friction can be observed. While the static friction coefficient decreases with increasing temperature, the dynamic friction coefficient reaches a minimum at approximately 100 °C. A normal pressure of about 0.002 N/mm² and a relative velocity of 19 mm/s were used for this investigation (Vishtal *et al*. 2014). The tribological conditions in friction tests of paperboard often do not cover the typical load spectrum of paperboard forming because the tests are targeted at other processes.

Fundamental investigations of the deep drawing of paperboard with rigid tools were carried out by Scherer (1935). The maximum drawing ratio can be increased by applying a controlled blank-holder-system and heated tool sections (Hauptmann 2010). Adapted forming processes, such as the hydroforming of paperboard, have displayed further enhancement of its formability (Östlund *et al*. 2011; Post *et al*. 2011; Groche *et al*. 2012).

Current deficits in constitutive modelling necessitate product and process designs for paperboard which are mainly based on trial-and-error approaches. The lack of methods to predict process limits has hampered the development of improved forming technologies. The aim of the present investigation was to adapt known design strategies and characterisation methods for metal to paperboard and evaluate the reliability of these methods for the prediction of paperboard forming processes.

CONSTITUTIVE MODELS

The subsequently described investigations were carried out with commercially available uncoated paperboard (two layer paperboard). It consists of recycled cellulose and has a specific volume of 1.3 to 1.45 cm³/g (~ 500g/m²). The thickness depends on the

moisture content and varies between 0.65 and 0.72 mm. Tensile tests were performed with a testing velocity of 10 mm/min. The elongation was measured by a video-extensometer (built-in video-extensometer of the tensile test machine by the company Zwick). Furthermore, the behaviour under uniaxial compression was investigated. The dimensions of the surfaces and thicknesses were determined before and after the compression tests by an optical measurement system displayed in Fig. 2b and tactile measurements, respectively. The optical measurement system used two five-megapixel cameras with a slider distance of 600 mm and 995 mm to the stochastically patterned surface of the test specimen. A calibration plate of dimensions 145 mm x 170 mm and a 50 mm lens were used (Optical strain measurement system Aramis by GOM – GOM 2011). Figure 2a displays the yield loci for an isotropic material according to von Mises' assumptions (von Mises 1928) and the anisotropic behaviour according to Hill's yield condition for DC04 (1.0338) and paperboard. The direction of the highest tensile flow stress is defined as the 1-direction, which is the main direction of the fibres in the case of paperboard. It is obvious that paperboard tends to have significantly higher anisotropy, associated with the fibre orientation, than common deep drawing metal. Appropriate constitutive modelling of paperboard must consider this phenomenon.

Figure 2c shows the correlation between the thickness reduction and surface variation in the compression tests. All materials exhibit larger deviations from volume constancy for small strains. This could be a result of the levelling of the surface roughness as well as the influence of elastic deformation. With increasing deformation, DC04 exhibits the expected volume constancy behaviour. In the case of 6% moisture content, in equilibrium with the normal climate (23 °C, 50% relative humidity), the achievable strain is smaller compared to that at 15% moisture content. In relation to the forming process, the maximum normal pressure during the testing of paperboard is approximately 6 N/mm². Nevertheless, considering a thickness of 651 ± 8 µm and an arithmetic mean roughness, R_a, of 6.6 ± 0.5 µm, the measurement point at higher strain indicates compressible behaviour. Paperboard with 15% moisture content behaves similarly to DC04 but with a slightly higher gradient, which could be caused by drying effects and the corresponding coefficient of expansion. During drying, the coefficient of expansion is three times larger in the thickness direction than the maximum in-plane coefficient. The experimental findings indicate that volume constancy seems to be a reasonable assumption in constitutive models, at least for moisture contents above that of equilibrium within a normal climate.

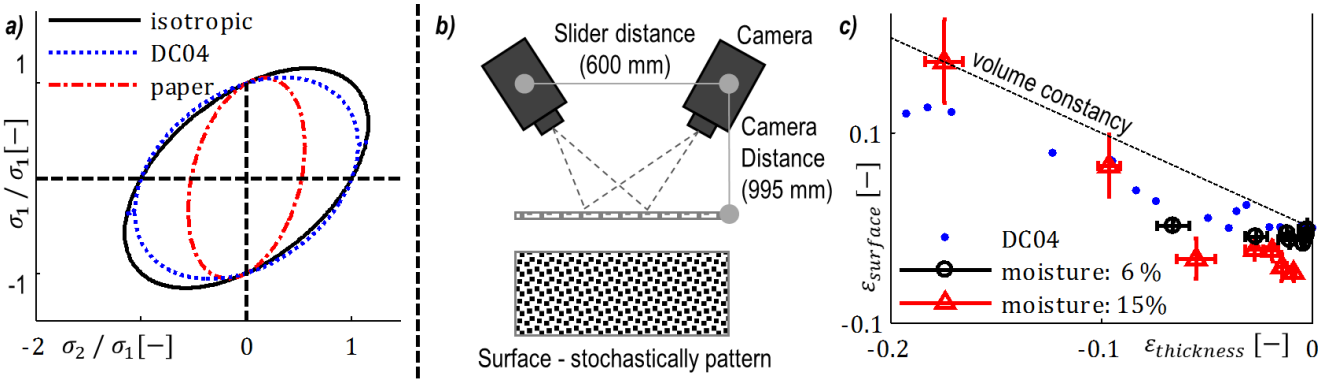

Fig. 2. a) Yield loci of isotropic, DC04, and paperboard material; b) measurement setup: optical surface measurement system; c) surface $\varepsilon_{surface}$ and thickness $\varepsilon_{thickness}$ strains in compression tests

FORMING LIMITS

To predict the producibility of a forming product, the limits of its formability must be examined. In sheet metal forming, it is common to describe process boundaries using forming limit diagrams (FLD). To develop these diagrams, different ratios of major and minor strains are determined by the use of different test setups and geometries. In this context, the major strain is the maximum surface strain and the minor strain is the perpendicular strain. The plot of the fracture points in a major-minor strain diagram enables the definition of forming limits. Strain distributions below the forming limit line are producible. Strain distributions near or higher than the forming limit line indicate that the product will fail during the forming process. The forming limits of paperboard are investigated according to test procedures well-established for the characterisation of metals (Burschi *et al*. 2014). More precisely, Table 1 and Fig. 3a display the test setup and geometry, respectively.

Table 1. Geometrical Data

	g_a	g_b	g_c	G_{var} (mm)			
	(mm)	(mm)	(mm)	G_0	G_1	G_2	G_3
TS1	12.5	70	-	-	-	-	-
TS2	20	3	36	25	50	100	-
TS4	30	20	60	plate	20	80	-
TS5	60/60/50	20	60	plate	10	15	22.5/10

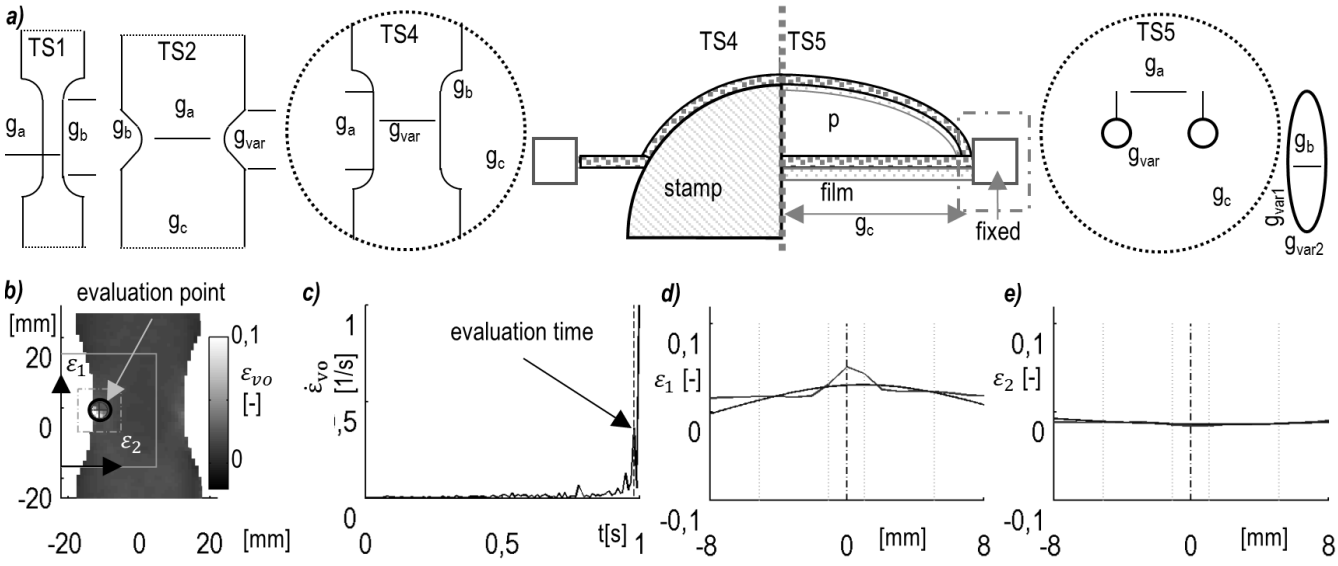

Fig. 3. a) Test setup and geometries; b) surface strain at fracture; c) definition of fracture time by strain rate diagram; d) calculation of ε_1 strain by a parabola fit according to ISO 12004; e) strain calculation in case of ε_2 strain

Ordinary tensile tests, tensile tests with notched samples, and Nakazima (Nakazima *et al.* 1971) tests were carried out. Additionally, bulge tests with a carrying layer and perforated samples, as proposed by Banabic *et al*. (2013), were performed. An optical surface measurement system (Aramis by GOM, Germany) was used for online strain measurement. Figure 3b displays the surface strain at the point of fracture. This

permits detection of the origin of the fracture. The strain rate-time diagram (Fig. 3c) of the selected surface point enables characterisation of the beginning of the fracture process. Both the fracture origin and the time at which the fracture begins are used to define the strain in the ε_1 and ε_2 directions by a fitted parabola, *e.g.* Fig. 3d/e. Local inhomogeneity and strain peaks are neglected by this approach. This allows the calculation of an ε_1-ε_2 relation. The use of the ε_1-ε_2 relation instead of the common major and minor strain seems advantageous for paperboard because of the anisotropy of the material.

The adopted bulge test offers the opportunity to adjust the state of strain by changing the geometry of the perforation. However, the proposed geometry fracture does not occur at the dome's pole. Further modification of the geometry could avoid this problem. The geometry of the die is given as a diameter of 120 mm and a chamfer of 8 mm. The influence of hydrostatic pressure on the forming limit is explored by hydraulic bulge tests with samples in a metal-paperboard-metal layer structure. Metal layers separate the paperboard from the fluid and lead to counter pressure.

Because the failure behaviour exhibits a strong dependency on the load direction, a classical forming limit diagrams (FLD), based on major and minor strain, is not suitable. Instead, an orientation-based forming limit diagram (OBFLD) is used and is displayed in Fig. 4. As a replacement for the major and minor strain diagram, the strain in the 0° and 90° directions of the material inside the fracture zone is evaluated. As can be seen from the OBFLD, the applied procedures result in similar ultimate strain combinations. Notched samples lead to negative values of secondary strain. In comparison, the Nakazima and modified bulge test enable positive strain combinations. Bulge tests with an additional top metal layer allow for higher hydrostatic pressure and indicate drastically extended forming limits. The resulting superimposed counter pressure of about 2 N/mm² shifts the forming limit line to significantly higher strain values.

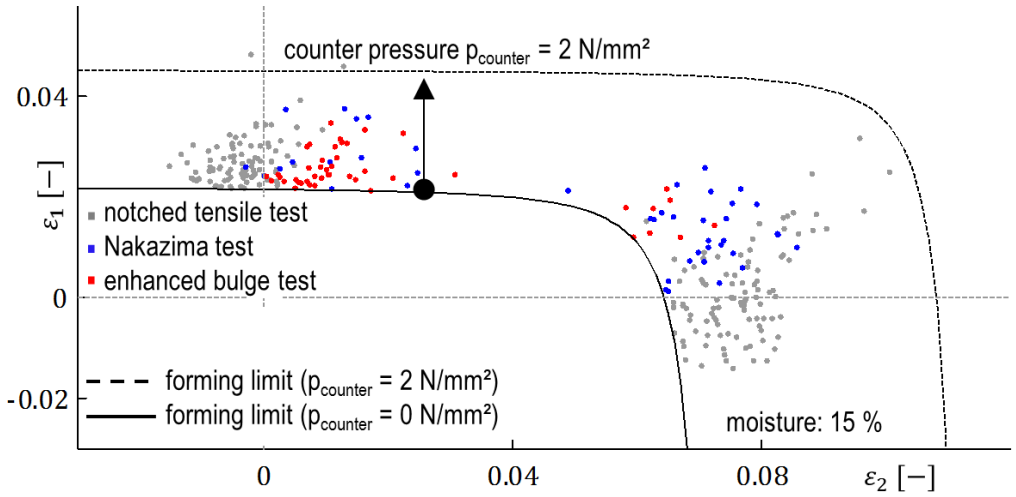

Fig. 4. Orientation based forming limit diagram (OBFLD)

FRICTION

A newly developed friction measurement device for paperboard forming was used to investigate the friction behaviour. It consists of a friction tool, heating units, and a

servo drive for controlled relative movement (Huttel *et al*. 2014). The paperboard forming process is characterised by short contact times, heated tools, and defined material moisture content. Furthermore, the friction behaviour of paperboard can be significantly affected by moisture, temperature, and relative velocity. This must be considered in friction measurements. Figure 5a displays the assembly of the friction measurement device. To minimise the effects of material drying before testing, the heated tools do not have any contact with the paperboard material before testing. The effect of heat transfer is displayed well in Fig. 5b. A paperboard is split at the half of the thickness of the sample and 0.08 mm thick sensor is inserted. A significant increase in the material's temperature after contact with the friction measurement tools can be seen. Similar effects can be expected in forming processes.

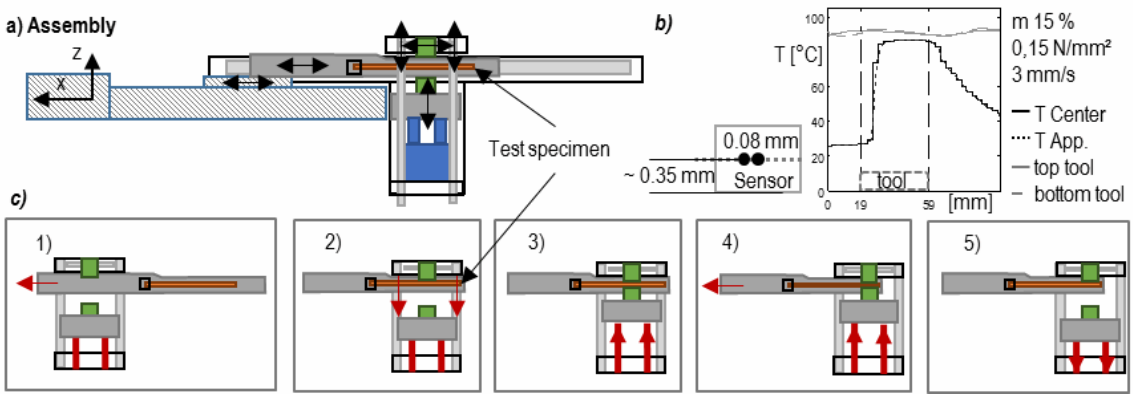

Fig. 5. Friction measurement device: a) assembly; b) temperature effects; c) measurement sequence

Figure 5c shows the measurement sequence. At the beginning of the process, the material is placed in the friction measurement device. The test specimen moves in the x-direction and the upper tool is lowered by a cam plate. Afterwards, the lower tool is moved against the upper tool by pneumatic pistons and normal force is applied. The friction test is performed at a predefined velocity. Within these investigations, five samples with a combined measurement length of 600 mm are used for the determination of each friction value.

Figure 6a shows friction coefficients for DC04 and tools made of cast iron 0.7060, as well as paperboard with tools made of tool steel 1.2085, at various testing velocities. With increasing velocity, DC04, and oil as the lubricant, friction tended to decrease. The friction behaviour of paperboard varied across a larger range. Increased temperature leads to reduced friction coefficients. A reduction of the moisture content decreased friction. Low moisture content tended to increase friction with velocity. This was reversed in the case of higher moisture content, as can be seen for 15% moisture content at room temperature (RT) and 90 °C. Test specimens at 140 °C displayed the same tendency as low-moisture content samples, which was possibly due to drying during the tests. Explanations for the variation of the friction coefficient by temperature and moisture can be given by the paperboard components. For example, the softening point of lignin, a part of paperboard, depends on the moisture content. Furthermore, water can form a vapour layer between the tools.

Figure 6b displays the water content of the material after testing with a material setup of 6% and 15% moisture. To measure the moisture content after testing, a part of

the sample was cut out (time less than 2 seconds) and the weight was measured. After this, the material was dried at 105°C to get the dry weight. This made it possible to calculate the moisture content right after the friction test procedure with heated tools. It can be seen that a testing temperature of approximately 140 °C led to a drying of the material to 0% moisture. This exemplifies the need for separation of the sample and friction measurement tool before the start of the testing process. The change in moisture content before testing can significantly change the determined friction.

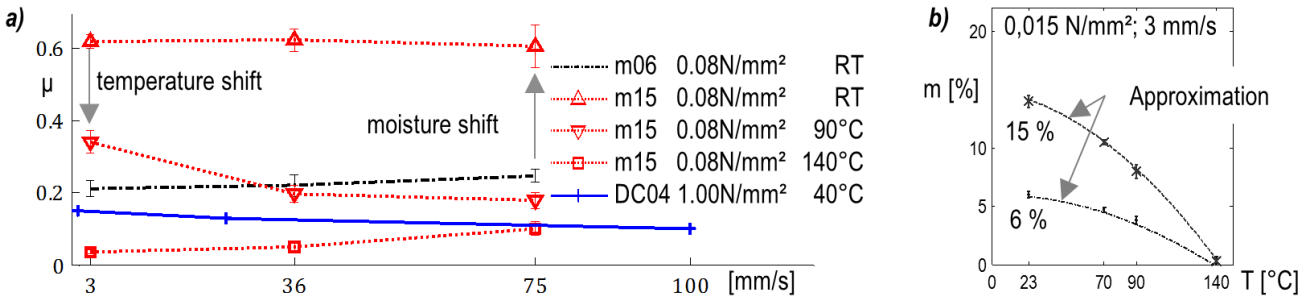

Fig. 6. a) Friction for DC04 (Filzek 2006) (tool material: 0.7060; lubricant: oil; and paperboard (tool material: 1.2085; lubricant: none; b) tool temperature – material – moisture – interaction

TECHNOLOGY

The previously described forming properties of paperboard show the need for control of temperature, moisture, and hydrostatic pressure during forming processes. Forming tools designed to meet these requirements are displayed in Fig. 7. Process 1 is a gas hydroforming process in which a film is used to separate the paperboard from the pressurised air. The blank-holder is controlled and can be heated. Process 2 makes use of a liquid for the forming process. A counter pressure can be applied. It has two functions: support of the material during the forming process and inhibition of wrinkling of the paperboard. This flexible blank-holder enables the material to flow from the outer area such that wrinkles can be suppressed. Abaqus (v. 6.12) was used to simulate the forming process. The dimensions of the forming tool and assembly are presented in Fig. 7c. The material behaviour is represented by Hill's flow function, as shown in Fig. 2. The mesh consists of two elements in the thickness direction with an edge ratio of three. A dynamic implicit (Hilber-Hughes-Taylor-Integration) solver is used.

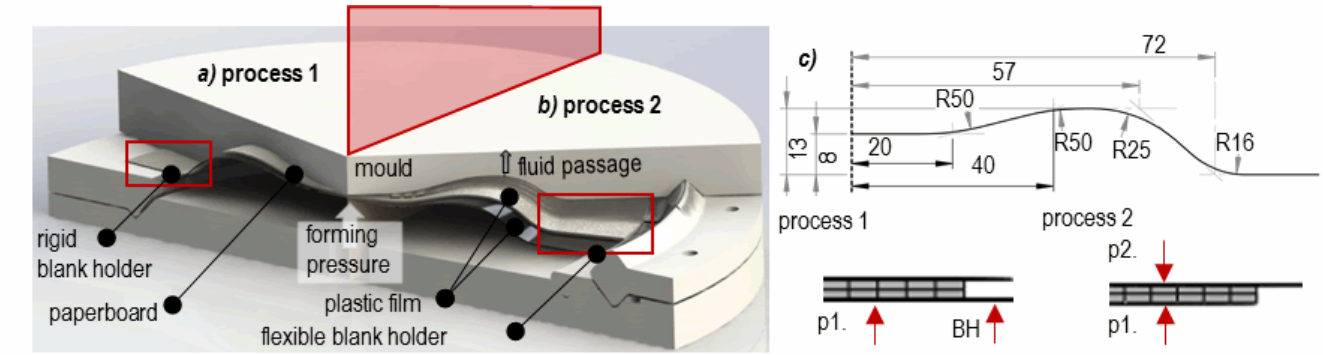

Fig. 7. Forming tool, geometry and FEA setup (Huttel and Groche 2014), a) process 1, b) process 2 with hydrostatic pressure support, c) geometry and FEA

Material data and the paperboard-tool interaction properties described in the previous sections form the basis for the numerical simulations of the forming processes. Figure 8a displays the comparison between the FEA (Finite Element Analysis) and experimental investigations based on the surface strain determination according to Eq. 1,

$$\varepsilon_{vo}=(\varepsilon_{11}^2+\varepsilon_{22}^2)^{0.5} \quad (1)$$

The strain distributions on the surfaces are transferred into the OBFLD. In the case of Forming Process 1, with 15% moisture content at RT, the FEA investigations in Fig. 8b predict that the material will fail during the forming process. This was confirmed by the experimental results shown in Fig. 8a. A change of the tool temperature affects, among other things, the coefficient of friction and thus, the surface strain distribution, as presented in Fig. 8b. In the case of the 140 °C and 200 N blank-holder force, a product without fracture was predicted. An increase of the blank-holder-force to 1000 N led to crossing of the forming limit (f_o) but not the fracture limit (f_r) in the OBFLD (see Fig. 8c). This implies that the process conditions were in a range in which failure could occur for some material batches. Figure 8d displays the surface failure occurring in the experimental investigation. The numerical material description considers a change of friction and a change of the initial material properties in the blank holder area as a result of drying processes. Furthermore, the drying of the whole material after the forming process is simulated by moisture-strain relations.

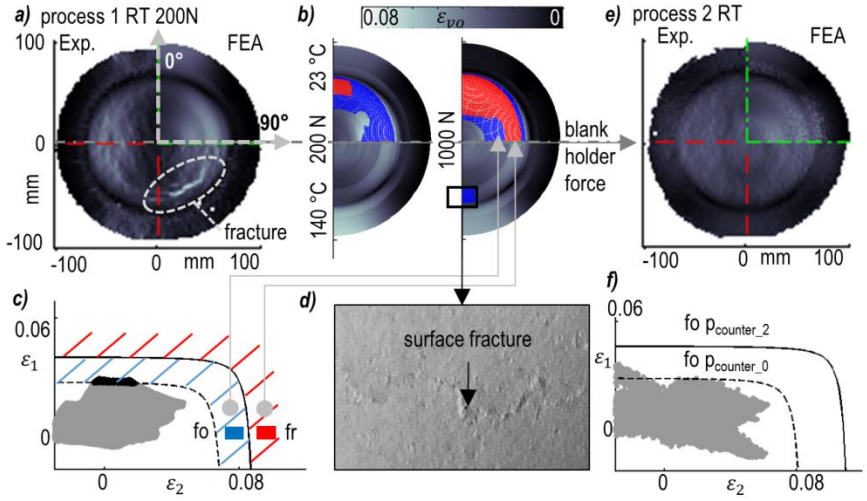

Fig. 8. Experimental and numerical investigation of the forming limit: a) Process 1: 200 N blank-holder force (bhf), b) numerical simulation of the failure behaviour, c) OBFLD in case of 1000 N bhf, d) surface fracture, e) Process 2, f) OBFLD of Process 2

The influence of counter pressure on the forming limits was studied by means of Process 2. Identical material settings, temperatures, and tools as those in Process 1 were used. As can be seen from Fig. 8e, the formability of the material was considerably enhanced. Experimental and FEA results yielded fracture-free surfaces of the formed paperboard samples. The enhancement of the forming limits is represented in Fig. 8f. All surface strain combinations remained underneath the forming limit line for a hydrostatic pressure of 2 N/mm² (f_o $p_{counter\_2}$).

Comparisons of the geometric and mechanical quantities are displayed in Fig. 9. The comparison between the final geometries resulting from the experimental and numerical investigations for Process 1 at RT is presented in Fig. 9a. FEA predicts the final shape of the product with high accuracy. Differences can be seen at the edge of the geometry. These can be affected by the drying process. Plane stress components in material direction 1 for cross sections of 0° and 90° are displayed in Fig. 9b. In this respect, Processes 1 and 2 exhibited similarities. The reason for the different failure behaviours in Processes 1 and 2 is visible in Fig. 9c. The stress components in the z or thickness directions differ because of the counter pressure superimposed in Process 2.

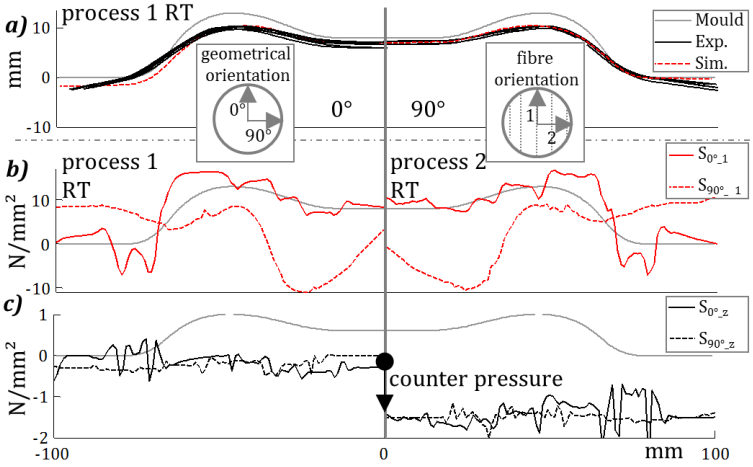

Fig. 9. Experimental and numerical investigation of the forming process (Huttel and Groche 2014): a) comparison of the geometry; b) stress in 1 direction; c) stress in z direction

DISCUSSION

Differences between metal and paperboard are most distinct with respect to their anisotropy and the sensitivity of the material and friction properties on changes in moisture content and temperature. Nevertheless, adapted characterisation, simulation, and design methods are widely transferrable from metal to paperboard. Additionally, the drying of paperboard after forming must be carefully considered to predict the final paperboard geometry accurately. Process design can be carried out with the material data gained. Superposed counter pressure is a suitable measure to effectively reduce failure probability.

Based on these findings, forming processes for paperboard can be systematically developed. Figure 10 displays an example of a process design aiming for producible product geometry. Starting with an initial design, wrinkles and fracture are detected (*e.g.*, Fig. 8a).

In the next step, wrinkles are minimised by geometry adaption and modified material orientation (Fig. 10b). The OBFLD displays fracture areas. This enables the adaptation of geometry to achieve a sound product (Fig. 10c). The final process design step is experimental verification.

Figure 10d shows the result: a product without wrinkles or fracture. This shows that an FEA-based design strategy for paperboard has the capability to develop systematically producible products made of paperboard.

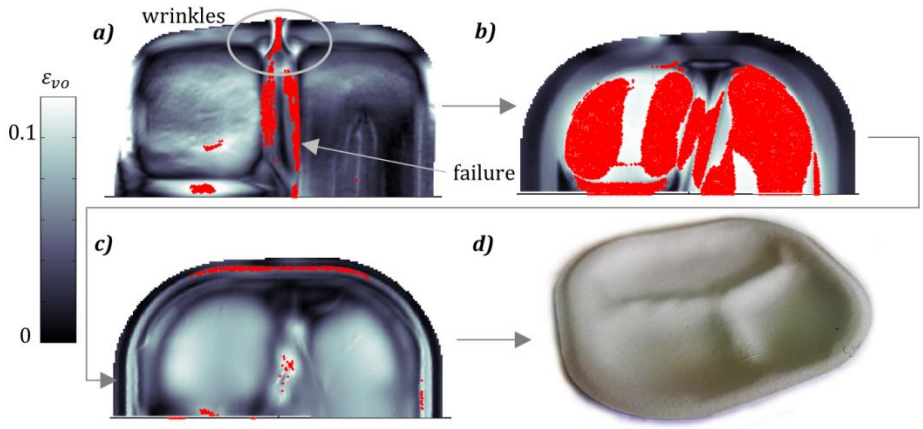

Fig. 10. Design strategy for the development of paperboard products: a) starting geometry, b) suppressed wrinkles, c) optimised result, d) final product

CONCLUSIONS

1. Formed products made of paperboard are highly attractive from mechanical and environmental viewpoints.
2. However, because of their fibrous structure, well-established modelling, testing, and design approaches used in metal forming can hardly be used.
3. Paperboard's behaviour and tribological conditions are strongly dependent on its moisture content and temperature. Both influencing parameters must be considered in process modelling and process design.
4. The formability of paperboard can be increased drastically by superimposed hydrostatic pressure.
5. Well-adjusted process conditions enable high plastic deformation.
6. These conditions can be used to form environmentally sound products by deep and stretch drawing. New products, as well as new areas of application for paperboard, are within reach.

ACKNOWLEDGMENTS

The presented investigations were carried out within the research projects GR1818/37-1 and IGF–17788N. The authors wish to thank the German Research Foundation (DFG), the Federal Ministry for Economic Affairs and Energy (BMWI), and the German Federation of Industrial Research Associations (AiF) for supporting the projects.

REFERENCES CITED

Alava, M., and Niskanen, K. (2006). "The physics of paper," *Reports on Progress in Physics* 69, 669-723. DOI:10.1088/0034-4885/69/3/R03

Back, E. L. (1991). "Paper-to-paper and paper-to-metal friction," *International Paper Physics Conference*, Kona, Hawaii, p. 49-65.

Banabic, D., Lazarescu, L., Paraianu, L., Coibanu, I., Nicodim, I., and Comsa, D. S. (2013). "Development of a new procedure for the experimental determination of the forming limit curves," *CIRP Annals - Manufacturing Technology* 62(1), 255-258. DOI: 10.1016/j.cirp.2013.03.05

Bruschi, S., Altan, T., Banabic, D., Bariani, P. F., Brosius, A., and Cao, J. (2014). "Testing and modelling of material behaviour and formability in sheet metal forming," *CIRP Annals - Manufacturing Technology* 63(2), 727-749. DOI: 10.1016/j.cirp.2014.05.005)

Davidson, R. W. (1972). "The weak link in paper dry strength," *TAPPI Journal* 55(4), 567-573.

Filzek, J. (2006). "Tribologische Prozessoptimierung als externe Dienstleistung," *9. Umformtechnisches Kolloquium Darmstadt*, Verlag Meisenbach, Bamberg, p. 161-170.

GOM mbH - Gesellschaft für Optische Messtechnik. Benutzerhandbuch – Aramis v6.3; 2011.

Groche, P. Huber, R., Dörr, J., and Schmoeckel, D. (2002). "Hydromechanical deep-drawing of aluminium-alloys at elevated temperatures," *CIRP Annals - Manufacturing Technology* 51(1), 215-218. DOI:10.1016/S0007-8506(07)61502-9

Groche, P., Huttel, D., Post, P., and Schabel, S. (2012). "Experimental and numerical investigation on the hydroforming behavior of paperboard," *Production Engineering* 6(3), 229-236. DOI 10.1007/s11740-012-0365-y

Hauptmann, M. (2010). *Die Gezielte Prozessführung und Möglichkeiten zur Prozessüberwachung beim mehrdimensionalen Umformen von Karton durch Ziehen*, PhD thesis, Institut für Verarbeitungsmaschinen und Mobile Arbeitsmaschinen, TU Dresden, Dresden, Germany.

Hill, R. (1948). "A theory of the yielding and plastic flow of anisotropic metals", *Proceedings of the Royal Society of London Series A-Mathematical and Physical Sciences*, 193(1033), 281-297. DOI: 10.1098/rspa.1948.0045

Huang, H. (2013). *Numerical and Experimental Investigation on Paperboard Converting Processes*, Ph.D. thesis, Department of Solid Mechanics, KTH, Stockholm, Sweden.

Huttel, D., and Groche, P. (2014). "New hydroforming concepts for sustainable fiber material (paperboard)," *International Conference New Developments in Hydroforming*, Fellbach, Germany, 127-141.

Huttel, D., Groche, P., May, A., and Euler, M. (2014). "Friction measurement device for fiber material forming processes," *Advanced Materials Research* 966-967, 65-79. DOI: 10.4028/www.scientific.net/AMR.966-967.65

Isaksson, P., Hägglund R., and Gradin, P. (2004). "Continuum damage mechanics applied to paper," *International Journal of Solids and Structures* 41(16-17), 4731-4755. DOI: 10.1016/j.ijsolstr.2004.02.043

Isaksson, P., Gradin, P., and Kulachenko, A. (2006). "The onset and progression of damage in isotropic paper sheets," *International Journal of Solids and Structures* 43(3-4), 713-726. DOI: 10.1016/j.ijsolstr.2005.04.035

ISO 12004. (2008). "Metallische Werkstoffe - Bleche Bänder - Be-stimmung der Grenzformänderungskurve, Deutsche Fassung EN ISO 12004," Deutsches Institut für Normung, Berlin.

Jiménez-Caballero, M. A., Conde, I., García, B., and Liarte, E. (2009). "Design of different types of corrugated board packages using finite element tools," *SIMULIA Customer Conference*.

Lemaitre, J., and Desmorat, R. (2005). *Engineering Damage Mechanics Ductile, Creep, Fatigue and Brittle Failures*, Springer, Berlin.

Mäkelä, P., and Östlund, S. (2003). "Orthotropic elastic–plastic material model for paper materials," *International Journal of Solids and Structures* 40(21), 5599-5620. DOI: 10.1016/S0020-7683(03)00318-4

Nakazima, K., Kikuma, T., and Hasuka, K. (1971). "Study on the formability of steel sheets," Ya-wata Technical Report (284).

Nygårds, M., Just, M., and Tryding, J. (2009). "Experimental and numerical studies of creasing of paperboard," *International Journal of Solids and Structures* 46(11-12), 2493-2505. DOI:10.1016/j.ijsolstr.2009.02.014

Östlund, S., Östlund, M., and Borodulina, S. (2011). "3D-forming of double-curved paperboard structures for packaging applications," *Poster Presented in Paper Physics Seminar*, Graz, Austria.

Post, P.-P., Huttel, D., Groche, P., and Schabel, S. (2011). "Paper characteristics influencing the deep drawing ability of paper," *Progress in Paper Physics Seminar*, Graz, Austria.

Scherer, K. (1935). *Das Ziehen von Pappe: Untersuchungen über die Ziehfähigkeit und den Ziehvorgang von Pappe*, Papier-Zeitung Verlagsgesellschaft mbH, Berlin, Germany.

Vishtal, A., Hauptmann, M., Zelm, R., Majschak, J.-P., and Retulainen, E. (2014). "3D forming of paperboard: The influence of paperboard properties on formability," *Packaging Technology and Science* 27(9), 677-691. DOI: 10.1002/pts.2056

Von Mises, R. (1928). "Mechanik der plastischen Formänderung von Kristallen," *Zeitschrift für angewandte Mathematik und Mechanik* (8), 161-185.

Weißbach, W. (2007). *Werkstoffkunde - Strukturen, Eigenschaften, Prüfung*, Vol. 16., Vieweg and Sohn Verlag, Wiesbaden, Germany.

Xia, Q. S. (2002). *Mechanics of Inelastic Deformation and Delamination in Paperboard*, PhD thesis, Dept. of Mechanical Engineering, Massachusetts Institute of Technology, Boston, MA.

Article submitted: May 6, 2015; Peer review completed: July 30, 2015; Revised version received: December 16, 2015; Accepted: December 17, 2015; Published: January 7, 2016.
DOI: 10.15376/biores.11.1.1855-1867